Molecular dynamics simulation of fabrication of Ni-graphene composite: temperature effect

Liliya L. Safina[1], *Julia A. Baimova*[1,2] ✉

[1]*Bashkir State University, Ufa 450032, Russia*
[2]*Institute for Metals Superplasticity Problems of RAS, Ufa 450001, Russia*
✉ *E-mail: julia.a.baimova@gmail.com*

Published in Micro & Nano Letters; Received on 18th July 2019; Revised on 18th November 2019; Accepted on 29th November 2019

Fabrication of Ni-graphene composite by hydrostatic pressure at finite temperatures or by the subsequent annealing is studied by molecular dynamics simulation. Crumpled graphene – the network of folded and crumpled graphene flakes connected by van-der-Waals bonds – is chosen as the matrix for Ni nanoclusters. It is found that hydrostatic compression at zero or room temperature cannot lead to the formation of the composite structure. Even strongly compressed crumpled graphene after unloading returned to the initial state of separated graphene flakes. However, annealing of the compressed structure at high temperature leads to the appearance of the valent bonds between neighbouring flakes. Simultaneously, hydrostatic compression at high temperature between 1000 and 2000 K leads to the better mixing of Ni atoms inside the structure and to the formation of strong covalent bonds between neighbouring flakes.

1. Introduction: Recently, metal-graphene nanostructures are considered as promising materials for various applications. It was shown that some metals such as Ni, Pt, Pd and Ti can be easily attached to the carbon polymorphs [1–3]. Thus, such metals can be covered by graphene flakes (GFs) or inserted to the short nanotubes and then combined to the 3D composite structure where after special treatment separated GFs will be connected by covalent bonds and transform from sp^2 to sp^3 carbon matrix [4]. There is a tendency that nickel-coated graphene became crumpled instead of remaining flat [5].

Metal-graphene composites have low weight, high stiffness and superior mechanical properties which can play an important role in currently engineered materials [6–10]. Such composites can be fabricated on the basement of graphene or carbon nanotubes and metal matrix, but special attention is paid to the combination of Ni nanoparticles (NP) with carbon matrix [11–14]. Such composites can be obtained by anchoring various types of NPs to the surface of graphene sheets through both in-situ (e.g. growing the NPs on the graphene surface) and ex-situ (e.g. attaching premade NPs to the graphene surface) methods [15].

Considering Ni NPs as a filler for carbon structure is an important and interesting issue because nickel–graphene structures are regarded as promising advanced materials. Ni by itself was successfully used for the catalysis of carbon polymorphs growth [16, 17], fabrication of new carbon configuration like nanoscrolls [18, 19], transformation of graphene to fullerenes [20] to name a few. Addition of Ni to the carbon structure can considerably improve the properties of the resulting material. For instance, nickel films on graphene retain their stability even at very high temperatures up to 1800 K [21, 22]; Ni dopant improves mechanical properties of carbon nanotubes [2]; the possibility to obtain better supercapacitors by the combination of Ni foams and carbon structures is shown [23], and so on. Thus, study of various carbon-Ni nanostructures is of high interest.

Crumpled graphene which was obtained experimentally [24, 25] can be considered as an excellent media for Ni NPs since it is highly porous material with a high specific surface area about 3523 m^2/g. This structure consists of numerous crumpled GFs, connected by van-der-Waals bonds. GFs can be filled with Ni NPs to form the composite structure with improved properties. Difference between melting temperature of graphene [26–28] and Ni NPs [3, 29] allow to control the mixture of components and changing of the properties.

In this Letter, the way of fabrication of Ni-graphene composite is investigated by molecular dynamics simulation. Two possibilities are found – annealing after hydrostatic compression at zero or room temperature, or hydrostatic compression conducted at high temperatures.

2. Simulation details: In Fig. 1, the structural elements of the proposed composite system are presented with the final 3D system – the precursor for composite. Ni_{47} NP is embedded inside the GF. Since, the structure of crumpled graphene is composed of variously crumpled and folded GFs [24], to obtain a valuable model, a rolled tube structure is chosen to reproduce folded GF. Even at low temperatures it changes its shape and can be easily transformed into a realistic crumpled GF. In addition, the presence of Ni NP immediately changed the ideal rolled structure of GF.

Then, GF with NP repeated four times along x, y and z axes to obtain 3D structure. Finally, the model, reproducing the system of crumpled graphene mixed with the Ni NPs is obtained. This model is an imitation of experiment where crumpled graphene was obtained by the usual method [23, 25] and then mixed with the Ni NPs before additional treatment: Ni NPs should fill in the large pores of crumpled graphene. After that, separated structural elements can be processed by pressure under various temperature conditions and form a composite. Periodic boundary conditions are applied along all three dimensions. As it was previously shown [30, 31], the orientation of GFs cannot affect its mechanical properties. Moreover, in the present work, high-temperature treatment is considered, and at high temperatures GFs will randomly rotate during simulation.

One of the important issues is the size of the Ni NPs and the amount of Ni atoms in the system. This will affect not only the formation of the composite but also further influence its mechanical properties. Here, GFs composed of 252 carbon atoms and the total amount of carbon atoms in the system is $N_C = 16128$, while number of Ni atoms is $N_{Ni} = 3008$ and in total $N = 19136$. It should be mentioned that during model justification, three other systems were considered with $N_{Ni}^{case1} = 1344$; $N_{Ni}^{case2} = 4224$ and $N_{Ni}^{case3} = 4992$ at the same number of carbon atoms. As it was found, there is almost no difference between *case 2* and *case 3*: the size of the Ni NP is too big which prevents the formation of

doi: 10.1049/mnl.2019.0414

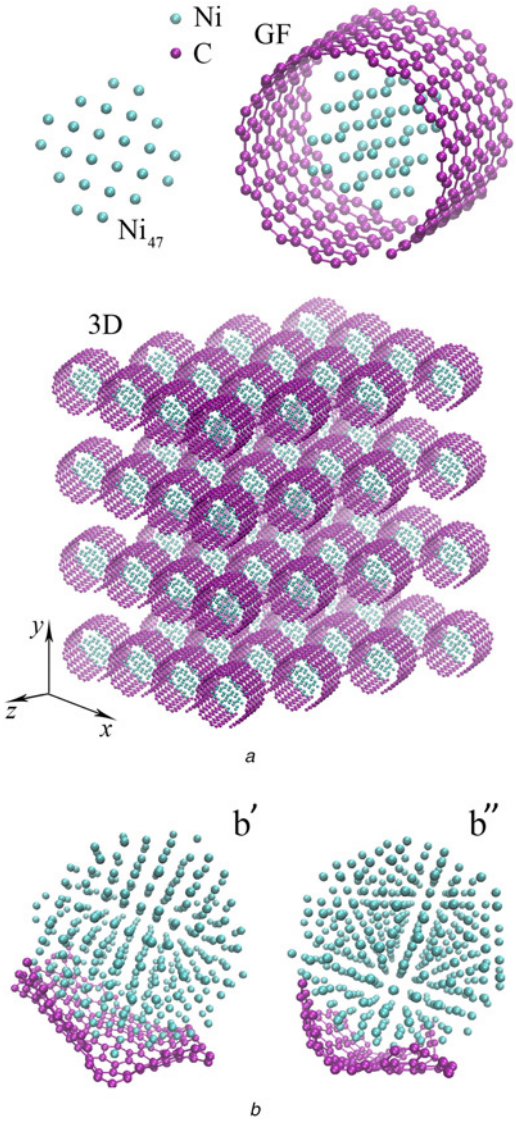

Fig. 1 *Structural state*
a Single Ni_{47} NP, GF with NP inside and 3D structure of crumpled graphene with NPs
b Structure after relaxation with Morse (*b′*) and ReaxFF (*b″*) potential

the composite. For *case 1* Ni atoms can be easily spread inside crumpled graphene, but properties of the obtained structure are close to the mechanical properties of pure crumpled graphene because the number of Ni atoms is too small. Thus, in the present work, only one case with $N_{Ni} = 3008$ is chosen to show the possibility of composite fabrication from the mixed Ni-graphene structure.

To fabricate composite, hydrostatic pressure (HP) at different temperatures $T = 0$, 300, 1000, 1500, 2000 K is applied to the initial ideal structure. Additionally, the effect of annealing is studied after hydrostatic compression at 0 K. The structure is exposed at $T = 300$, 1000, 1500, 2000 K during 20 and 100 ps to find the effect of different temperatures and annealing time.

For description of interatomic interactions two potentials are used – AIREBO for carbon–carbon interaction [32]

$$U_{\text{AIREBO}} = \frac{1}{2}\sum_{i}\sum_{i\neq j}\left[U_{ij}^{\text{REBO}} + U_{ij}^{\text{vdW}} + \sum_{k\neq i,j}\sum_{l\neq i,j,k} U_{kijl}^{\text{T}}\right], \quad (1)$$

where U_{ij}^{REBO} is the hydrocarbon REBO potential, U_{ij}^{vdW} term adds van-der-Waals interaction and U_{kijl}^{T} describes various dihedral angle preferences in hydrocarbon configurations and Morse for nickel–nickel and carbon–nickel interactions [33–35, 3]

$$U^{\text{Morse}}(r) = D[(1 - \mathrm{e}^{-\beta(r-r_e)})^2 - 1], \quad (2)$$

where D is the binding energy, r_e is the distance for potential energy minimum and β is the potential parameter. Application of AIREBO potential for studying of carbon structures was previously proved by numerous works for 2D [36, 37] and 3D [38–41] structures. Application of Morse potential for Ni–C interaction is a common method used to simplify the complex calculations. However, different sets of Morse parameters were developed according to the issues investigated [42, 34, 35, 16]. In the present work, parameters for interaction of graphene with Ni atoms obtained from *ab-initio* calculations [34, 35] are used. The parameters for the Ni–C Morse potential are $D = 0.433$ eV, $r_e = 2.316$ Å and $\beta = 3.2441/$Å, indicating a van der Waals type bonding between Ni and graphene. In [3], it is shown that such potential parameters can be successfully used for the description of different carbon polymorphs with Ni nanoclusters. Moreover, results, obtained by molecular dynamics with recently developed ReaxFF (Reactive Force Field) [43–46, 18] are presented to additionally prove the applicability of Morse potential for Ni–C interaction. All the simulations are conducted in LAMMPS molecular dynamics simulator.

In Fig. 1*b*, structures after relaxation under Morse (*b′*) and ReaxFF (*b″*) potential are presented. As can be seen, Morse and ReaxFF potential reproduce the same structural state. However, the application of ReaxFF leads to a similar result for a significantly longer time than Morse. Therefore, ReaxFF is more suitable either for modelling small systems or for processes occurring during a short time. In the present work, fabrication of the composite structure composed of Ni NPs covered by GFs is considered. Thus, for the present goal, Morse potential with the chosen parameters suites well.

3. Results and discussion: Deformation behaviour of crumpled graphene can be described both by pressure–strain and pressure–density curves. The considered structure can be hydrostatically compressed until high densities. In Fig. 2*a*, pressure–density curves during hydrostatic compression at 0, 1000 and 2000 K are presented.

Here, $p = (\sigma_{xx} + \sigma_{yy} + \sigma_{zz})/3$, where σ_{xx}, σ_{yy} and σ_{zz} are stress components calculated during simulation. As it can be seen, HP at high temperatures leads to the decrease of critical pressure at achieving the same final density 6.5 g/cm^3. From the snapshots it can be seen that at 1000 K, structural elements can change its shape, freely rotate, covalently connect to each other. Moreover, at this temperature Ni NPs can be easily compressed by GFs, though NPs are not melted yet and separated Ni atoms do not move outside the flakes. Heated Ni NP became soft, while at these temperature GFs are very rigid and under compression can affect the shape of the NPs. Thus, Ni NPs of this size at 1000 K can be compressed due to the deformation of GFs. Changing of the initial shape lead to the better placing and compacting of structural units.

To check the mechanical response of the compressed structure, its tensile behaviour is discussed further. In Fig. 3*a*, pressure–strain curves during tension are presented for crumpled graphene hydrostatically compressed at 0, 1000 and 2000 K. The increase in temperature leads to a considerable decrease in critical stresses. This can be explained by the temperature effect: temperature increase leads to better relaxation of stresses accumulated during HP since compression is conducted to very high densities. Here, to find if the composite was obtained, better to evaluate the course of the curves than pressure values. A slight decrease in the pressure after $\varepsilon = 0.3$ corresponds to the formation of

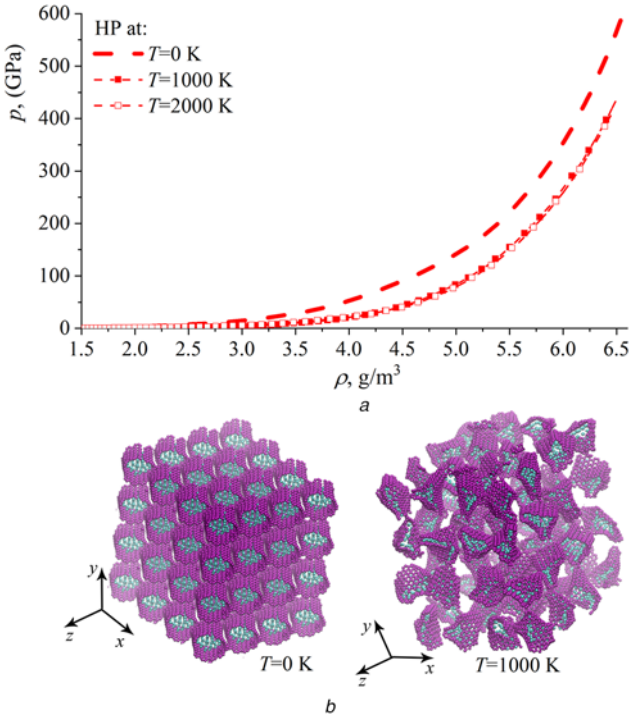

Fig. 2 *Effect of hydrostatic compression*
a Pressure–density curves under hydrostatic compression at 0, 1000 and 2000 K
b Snapshot of the structure at hydrostatic strain $\varepsilon = 0.1$ for two temperatures

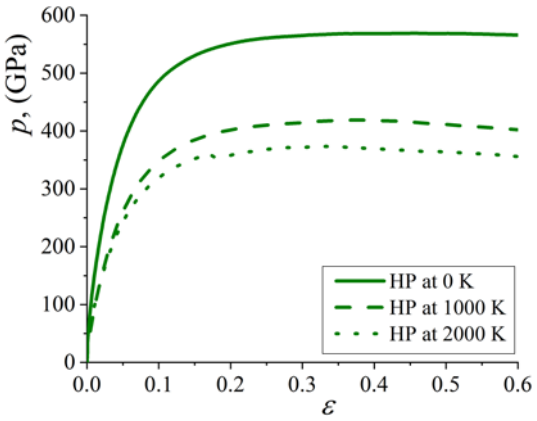

Fig. 3 *Pressure–strain curves under tension for crumpled graphene hydrostatically compressed at 0, 1000 and 2000 K*

the composite structure. At high temperatures, the appearance of new covalent bonds between GFs is facilitated. Rotation of the structural elements during compression allows their better stacking.

Hydrostatic compression can be easily realised at room temperature, but such a considerable increase of temperature to 1000 K or even 2000 K significantly complicate the task. Next way to facilitate the formation of the new covalent bonds is annealing after HP at 0 K or room temperature. In Fig. 4, HP as the function of strain is presented for tension after HP at 0 K and HP followed by annealing at 1000 and 2000 K. The tensile simulations after annealing during 20 and 100 ps is conducted in order to find the optimised annealing time for this model; the results are shown in Fig. 4*a*. Two curves almost coincide which means that 20 ps is quite enough time. Thus, in Fig. 4*b*, pressure–strain curves after annealing during 20 ps are presented.

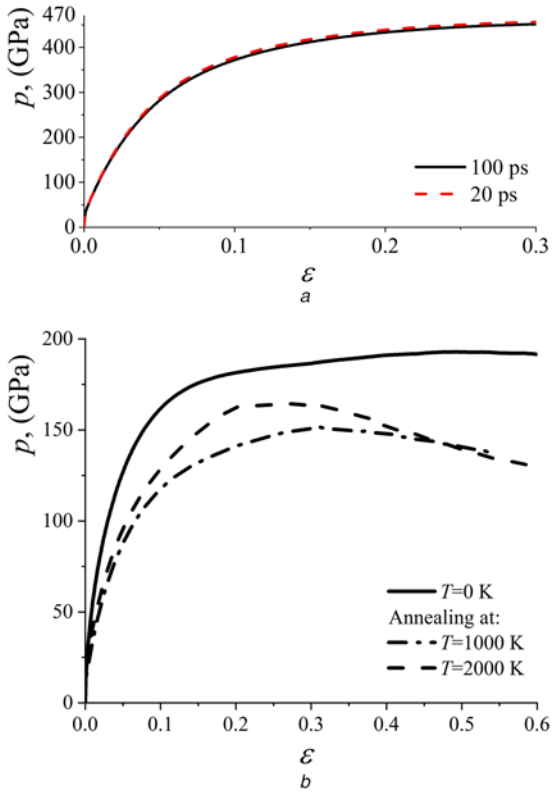

Fig. 4 *Pressure-strain curves*
a Pressure–strain curves under tension after annealing at 1000 K during 20 and 100 ps
b Pressure–strain curves under tension for crumpled graphene hydrostatically compressed at 0 K and annealed at 1000 and 2000 K

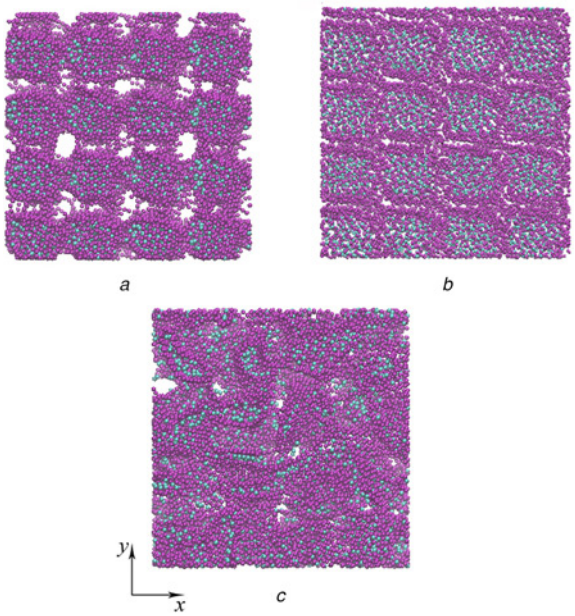

Fig. 5 *Snapshots of the structure*
a Snapshots of the structure at tensile strain $\varepsilon = 0.6$ after hydrostatic compression at 0 K
b Annealed at 1000 K
c After hydrostatic compression at 1000 K

At the initial strains, the curves increase almost linearly. For structure hydrostatically compressed at 0 K, an increase of p is found until high values of strain. In this case, structural elements

doi: 10.1049/mnl.2019.0414

are separate, no formation of new covalent bonds is found. Comparatively, for structure annealed at 2000 K decrease of HP took place after $\varepsilon = 0.2$ and for structure annealed at 1000 K – at $\varepsilon = 0.3$.

In Fig. 5, snapshots of the final structures after tension to $\varepsilon = 0.6$ obtained at different conditions are presented. From Fig. 5*a* it is clearly seen that structural units are separated and can be easily returned to the initial state. For structures compressed at high temperature or after annealing, pores are much smaller. Better mixing of the elements is seen. Individual GFs still can be seen in the structure, but a lot of new covalent bonds appeared during high-temperature treatment. Nearest neighbours analysis showed that most of the carbon atoms change its hybridisation from sp^2 to sp^3. Better mixing is obtained when high temperature was applied during hydrostatic compression.

4. Conclusions: In summary, the effect of hydrostatic compression at final temperatures and annealing on the formation of Ni-graphene composite is studied by molecular dynamics. It is observed that even high pressure up to 500 GPa cannot be successfully used to obtain monolith composite structure. Only heating to high temperatures close to 1000 K and higher can result in the transformation of GFs and formation of covalent bonds between neighbouring structural elements.

Present work revealed that special high-temperature treatment is an efficient way of fabrication of metal-carbon nanocomposites. In frames of the present work, only the pressure–strain curves and structural states of the material obtained after different treatment are discussed. However, further study confirming the formation of composite structure is required, for example, calculation on its Raman effect [47] which are planned to be done further. This study can be continued by further changing of the temperature regimes or by mixing various external conditions. Obtained results open new opportunities for fabrication of composites with improved mechanical properties.

5. Acknowledgment: Calculation of the hydrostatic compression of CG is done by J.A.B. and is supported by the program of Fundamental Researches of Government Academy of Sciences of IMSP RAS. Investigation of hydrogenated CG is made by L.R.S. and is supported by the Grant of the President of the Russian Federation for state support of young Russian scientists – doctors of sciences grant no. MD-1651.2018.2.

6 References

[1] Park N., Sung D., Lim S., *ET AL.*: 'Realistic adsorption geometries and binding affinities of metal nanoparticles onto the surface of carbon nanotubes', *Appl. Phys. Lett.*, 2009, **94**, p. 073105
[2] Inoue S., Matsumura Y.: 'Influence of metal coating on single-walled carbon nanotube: molecular dynamics approach to determine tensile strength', *Chem. Phys. Lett.*, 2009, **469**, pp. 125–129
[3] Safina L.R., Baimova J.A., Mulyukov R.R.: 'Nickel nanoparticles inside carbon nanostructures: atomistic simulation', *Mech. Adv. Mater. Mod. Process.*, 2019, **5**, pp. 1–11
[4] Song H.-Y., Zha X.-W.: 'Mechanical properties of nickel-coated single-walled carbon nanotubes and their embedded gold matrix composites', *Phys. Lett. A*, 2010, **374**, pp. 1068–1072
[5] Hu Q.-H., Wang X.-T., Chen H., *ET AL.*: 'Synthesis of Ni/graphene sheets by an electroless Ni-plating method', *New Carbon Mater.*, 2012, **27**, pp. 35–41
[6] Neubauer E., Kitzmantel M., Hulman M., *ET AL.*: 'Potential and challenges of metal-matrix-composites reinforced with carbon nanofibers and carbon nanotubes', *Compos. Sci. Technol.*, 2010, **70**, pp. 2228–2236
[7] Shiozawa H., Briones-Leon A., Domanov O., *ET AL.*: 'Nickel clusters embedded in carbon nanotubes as high performance magnets', *Sci. Rep.*, 2015, **5**, p. 15033
[8] Hu Z., Tong G., Lin D., *ET AL.*: 'Laser sintered graphene nickel nanocomposites', *J. Mater. Process. Technol.*, 2016, **231**, pp. 143–150
[9] Jiang J., He X., Du J., *ET AL.*: 'In-situ fabrication of graphene-nickel matrix composites', *Mater. Lett.*, 2018, **220**, pp. 178–181
[10] Ji L., Chen F., Huang H., *ET AL.*: 'Preparation of nickel–graphene composites by jet electrodeposition and the influence of graphene oxide concentration on the morphologies and properties', *Surf. Coat. Technol.*, 2018, **351**, pp. 212–219
[11] Neiva E.G., Souza V.H., Huang K., *ET AL.*: 'Graphene/nickel nanoparticles composites from graphenide solutions', *J. Colloid Interface Sci.*, 2015, **453**, pp. 28–35
[12] Mahale N.K., Ladhe R.D., Attarde S.B., *ET AL.*: 'Synthesis and the structural transformation of fcc to hcp in Ni-graphene nanocomposite by simple chemical route via sonication', *J. Nanoparticles*, 2014, **2014**, pp. 1–7
[13] Fu Y., Cui W.J., Yan F., *ET AL.*: 'Synthesis of graphene load nickel nanoparticles composites with hydrothermal process', *Adv. Mater. Res.*, 2013, **760–762**, pp. 793–796
[14] Mahboobi S., Meghdari A., Jalili N., *ET AL.*: 'Molecular dynamics study of success evaluation for metallic nanoparticles manipulation on gold substrate', *Micro Nano Lett.*, 2010, **5**, p. 286
[15] Yin P.T., Shah S., Chhowalla M., *ET AL.*: 'Design, synthesis, and characterization of graphene–nanoparticle hybrid materials for bioapplications', *Chem. Rev.*, 2015, **115**, pp. 2483–2531
[16] Moseler M., Cervantes-Sodi F., Hofmann S., *ET AL.*: 'Dynamic catalyst restructuring during carbon nanotube growth', *ACS Nano*, 2010, **4**, pp. 7587–7595
[17] Kwon H., Ha J.M., Yoo S.H., *ET AL.*: 'Synthesis of flake-like graphene from nickel-coated polyacrylonitrile polymer', *Nanoscale Res. Lett.*, 2014, **9**, p. 618
[18] Bejagam K.K., Singh S., Deshmukh S.A.: 'Nanoparticle activated and directed assembly of graphene into a nanoscroll', *Carbon. N. Y.*, 2018, **134**, pp. 43–52
[19] Savin A.V., Korznikova E.A., Lobzenko I.P., *ET AL.*: 'Symmetric scrolled packings of multilayered carbon nanoribbons', *Phys. Solid State*, 2016, **58**, pp. 1278–1284
[20] Lebedeva I.V., Knizhnik A.A., Popov A.M., *ET AL.*: 'Ni-assisted transformation of graphene flakes to fullerenes', *J. Phys. Chem. C*, 2012, **116**, pp. 6572–6584
[21] Galashev A.E., Polukhin V.A.: 'Computer simulation of thin nickel films on single-layer graphene', *Phys. Solid State*, 2013, **55**, pp. 2368–2373
[22] Galashev A.E.: 'Computer simulation of the thermal stability of nickel films on two-layer graphene', *High Temp.*, 2014, **52**, pp. 633–639
[23] Zhou H., Liu D., Luo F., *ET AL.*: 'Preparation of graphene nanowalls on nickel foam as supercapacitor electrodes', *Micro Nano Lett.*, 2018, **13**, pp. 842–844
[24] Zhang L., Zhang F., Yang X., *ET AL.*: 'Porous 3D graphene-based bulk materials with exceptional high surface area and excellent conductivity for supercapacitors', *Nature*, 2013, **3**, p. 1408
[25] Chang C., Song Z., Lin J., *ET AL.*: 'How graphene crumples are stabilized?', *RSC Adv.*, 2013, **3**, p. 2720
[26] Ganz E., Ganz A.B., Yang L.-M., *ET AL.*: 'The initial stages of melting of graphene between 4000 K and 6000 K', *Phys. Chem. Chem. Phys.*, 2017, **19**, pp. 3756–3762
[27] Los J.H., Zakharchenko K.V., Katsnelson M.I., *ET AL.*: 'Melting temperature of graphene', *Phys. Rev. B*, 2015, **91**, p. 045415
[28] Orekhov N.D., Stegailov V.V.: 'Molecular-dynamics based insights into the problem of graphite melting'. Journal of Physics: Conf. Series, Kabardino-Balkaria, Russia, 2015, vol 653, p. 012090
[29] Verkhovtsev A.V., Schramm S., Solov'yov A.V.: 'Molecular dynamics study of the stability of a carbon nanotube atop a catalytic nanoparticle', *Eur. Phy. J., D*, 2014, **68** p. 246
[30] Baimova J.A., Liu B., Dmitriev S.V., *ET AL.*: 'Mechanical properties of bulk carbon nanostructures: effect of loading and temperature', *J. Phys. D, Appl. Phys.*, 2015, **48**, p. 095302
[31] Baimova J.A., Liu B., Dmitriev S.V., *ET AL.*: Mechanical properties of crumpled graphene under hydrostatic and uniaxial compression', *Phys. Chem. Chem. Phys.*, 2014, **16**, pp. 19505–19513
[32] Stuart S.J., Tutein A.B., Harrison J.A.: 'A reactive potential for hydrocarbons with intermolecular interactions', *J. Chem. Phys.*, 2000, **112**, pp. 6472–6486
[33] Girifalco L.A., Weizer V.G.: 'Application of the morse potential function to cubic metals', *Phys. Rev.*, 1959, **114**, pp. 687–690
[34] Katin K.P., Prudkovskiy V.S., Maslov M.M.: 'Molecular dynamics simulation of nickel-coated graphene bending', *Micro Nano Lett.*, 2018, **13**, pp. 160–164
[35] Galashev A.Y., Katin K.P., Maslov M.M.: 'Morse parameters for the interaction of metals with graphene and silicene', *Phys. Lett. A*, 2019, **383**, pp. 252–258
[36] Baimova J., Murzaev R., Rudskoy A.: 'Discrete breathers in graphane in thermal equilibrium', *Phys. Lett. A*, 2017, **381**, pp. 3049–3053

[37] Yang X., Wu S., Xu J., *ET AL.*: 'Spurious heat conduction behavior of finite-size graphene nanoribbon under extreme uniaxial strain caused by the AIREBO potential', *Phy. E, Low-dimensional Syst. Nanostructures*, 2018, **96**, pp. 46–53
[38] Murzaev R., Bachurin D., Korznikova E., *ET AL.*: 'Localized vibrational modes in diamond', *Phys. Lett. A*, 2017, **381**, pp. 1003–1008
[39] Pedrielli A., Taioli S., Garberoglio G., *ET AL.*: 'Designing graphene based nanofoams with nonlinear auxetic and anisotropic mechanical properties under tension or compression', *Carbon. N. Y.*, 2017, **111**, pp. 796–806
[40] Bai L., Srikanth N., Korznikova E.A., *ET AL.*: 'Wear and friction between smooth or rough diamond-like carbon films and diamond tips', *Wear*, 2017, **372–373**, pp. 12–20
[41] Krylova K.A., Baimova J.A., Mulyukov R.R.: 'Effect of deformation on dehydrogenation mechanisms of crumpled graphene: molecular dynamics simulation', *Lett. Mater.*, 2019, **9**, pp. 81–85
[42] Xu Z., Yan T., Ding F.: 'Atomistic simulation of the growth of defect-free carbon nanotubes', *Chem. Sci.*, 2015, **6**, pp. 4704–4711
[43] van Duin A.C.T., Dasgupta S., Lorant F., *ET AL.*: 'ReaxFF: A reactive force field for hydrocarbons', *J. Phys. Chem. A*, 2001, **105**, pp. 9396–9409
[44] Srinivasan S.G., van Duin A.C.T., Ganesh P.: 'Development of a ReaxFF potential for carbon condensed phases and its application to the thermal fragmentation of a large fullerene', *J. Phys. Chem. A*, 2015, **119**, pp. 571–580
[45] Li K., Zhang H., Li G., *ET AL.*: 'ReaxFF molecular dynamics simulation for the graphitization of amorphous carbon: A parametric study', *J. Chem. Theory Comput.*, 2018, **14**, pp. 2322–2331
[46] Nielson K.D., van Duin A.C.T., Oxgaard J., *ET AL.*: 'Development of the ReaxFF reactive force field for describing transition metal catalyzed reactions, with application to the initial stages of the catalytic formation of carbon nanotubes', *J. Phys. Chem. A*, 2005, **109**, pp. 493–499
[47] Nanda S.S., Kim B.J., Kim K.-W., *ET AL.*: 'A new device concept for bacterial sensing by Raman spectroscopy and voltage-gated monolayer graphene', *Nanoscale*, 2019, **11**, pp. 8528–8537

doi: 10.1049/mnl.2019.0414